Biomed Microdevices (2012) 14:739–750
DOI 10.1007/s10544-012-9655-6

Micromachined Coulter counter for dynamic impedance study of time sensitive cells

Yifan Wu · James D. Benson · Mahmoud Almasri

Published online: 25 April 2012

Abstract This paper describes the design, modeling, fabrication and characterization MEMS Coulter counter that can detect and monitor the dynamic cell impedance changes *in situ* as a function of time after mixing isolated cell populations with different extracellular media within 0.3 s from the start of mixing. The novelty of this design is the use of multi-electrodes with vertical sidewalls to enable the measurements of time sensitive cells with significantly enhanced sensitivity as well as the integration of passive mixing, focusing of cells in line and impedance detection using the vertical electrodes on a single chip that is made mainly using multilayer of SU-8, which has not been reported before. The devices were tested with both fluidic and electrical functionality using yeast cells in cryoprotectant agent (diluted dimethyl sulfoxide), red blood cells, microbeads with different dimensions, and dyed fluids. The results demonstrate rapid changes of cell volume within the first 0.6 s after mixing followed by a stable and a fixed cell volume. The micromixer was initially simulated using COMSOL finite element tool. Image processing technique was used to quantitatively evaluate mixing efficiency by analyzing color intensities variation of captured images of 2 dyed fluids mixed in the channel at flow rates between 0.1–0.4 μl/min, the mixing efficiencies were between 87 %–95 %, respectively.

Keywords Coulter counter · Time sensitive cell · Dynamic study of cell · Red blood cell · Yeast cells · BioMEMS

Y. Wu · J. D. Benson · M. Almasri (✉)
University of Missouri,
Columbia, MO, USA
e-mail: almasrim@missouri.edu

1 Introduction

Coulter counter is a standard diagnostic device for counting and sizing cells and particles widely used in laboratory medicine and pathology, clinical diagnostics, environmental monitoring, and food pathogen screening (Levin et al. 1980; Gast et al. 2006). These devices are used to perform rapid, accurate analysis of blood, colloidal particles, antigens, pollen and viruses, and other cells and tissues (England-Down 1975). Commercially available Coulter counters have a number of limitations. They are configured to require relatively large sample volume and severely limit measurement of time sensitive cell characteristics (e.g. changes in volume in response to changes in solute concentrations). The sample size and time constraints are detrimental to accurate dynamic volume measurements for some cell types. For example, red blood cells rapidly adjust volumetrically to anisosmotic environments making measurements of water and solute permeability parameters impossible with existing Coulter counter technology. Our counter is specifically designed to measure the cell impedance changes within 0.3 s from the start of mixing. This time delay is determined by the time scale of the water permeation process for specific cell types (Levin et al. 1980; Papanek 1978; Milgram-Solomon).

Several groups have successfully demonstrated miniaturized Coulter counters with various designs using micromachining technology (Larsen et al. 1997; Koch et al. 1999; Zhe et al. 2007; Ateya et al. 2008; Saleh and Sohn 2003). These miniaturized Coulter counters are designed to measure impedance of cells using one or two electrode pairs and thus may only be used for cell counting purposes and static cell sizing. In addition, these methods cannot accurately measure the impedance of cells with significantly different cell geometry such as platelets. Miniaturized Coulter counters provide many advantages including significantly

reduced sample volume, low cost, low power consumption, and portability (Koch et al. 1999). Currently, several groups have addressed many issues related to Coulter's channel clogging, detection techniques, sensitivity and throughput. Coulter counters generally employ a focusing mechanism to confine a small well- defined volume sample to the center of the channel to prevent clogging of the entrance of the Coulter channel, and an electrode pair for impedance measurement as a means for cell counting. The cells are focused horizontally into a tight stream, or liquid aperture, to the approximate size of the cell or beads by two high flow rate sheath fluid flows using two-dimensional hydrodynamic focusing (Scott et al. 2008; Tsai et al. 2008; Gawad et al. 2001; Sundararajan et al. 2004). Since the physical dimensions of the channel are much larger than the Coulter aperture, the use of hydrodynamic focusing prevents channel blocking, but there is the possibility of fluid diffusion. Another drawback is the need for an additional reservoir for the sheath flow medium which has to be kept free of dust and bacteria. To resolve this issue, other groups proposed to use air as a sheath fluid, which eliminates the complex maintenance of the liquid reservoirs (Ateya et al. 2008; Lin et al. 2004). However, this technique has a limited sensitivity since the top and bottom fluid path is not focused. 3-D hydrodynamic focusing solves this issue by vertically focusing the sample to a size comparable to the cell dimensions, thus preventing cell overlap in the vertical direction (Tsai et al. 2008; Sundararajan et al. 2004; Chang et al. 2007; Mao et al. 2007), and enhancing sensitivity. This technique enables the device to probe particles with a wide range of diameters. Dielectrophoresis (DEP) focusing the motion of the cells in the channel is regulated by the negative DEP force in the cross flow direction and combined with the hydrodynamic flow force in the flow direction (Holmes et al. 2006; Wang et al. 2006). This is more desirable because it does not need sheath flow.

Several cell and particle detection techniques including optical and electrical impedance sensing techniques were used. The former includes fluorescence detection using a fluorescent marker to facilitate their optical detection and counting (Chen and Wang 2009); fluorescence detection with micromachined fibers as a waveguide on the microchip (Bernini et al. 2006); and laser-induced fluorescence techniques (Chen and Wang 2008). The later technique is label-free and more adaptable to miniaturization. It includes DC impedance sensing, low frequency (100 kHz) AC impedance sensing and high frequency (above 100 kHz) AC impedance sensing (Zheng et al. 2008a, b, c). The DC impedance sensing was first invented by Wallace H. Coulter (Coulter 1953). This technique is accurate for electrodes with large size because it reduces the electrode-electrolyte impedance. In this case, the cell volume is the only factor that determines the measured system impedance. In the MEMS-based particle counter, electrodes are in the micrometer range and double-layer impedance must be taken into account since it is inversely proportional to the electrode area (Zheng et al. 2008a, b). Reducing the system sensitivity may also cause irreversible oxidation of electrodes (Zheng and Tai 2006). The AC measurement could solve oxidation and bubble problems. At low frequency, the impedance of the cell, which also includes the double layer capacitance, is mainly determined by its volume. It is important to note that the double layer capacitance decreases as the frequency increases. At higher frequency, the intracellular structure contributes to the overall measured impedance (Nieuwenhuis et al. 2004), and the double layer capacitance becomes comparable to the stray capacitance between the sensing electrodes. Thus, the operational frequency cannot go beyond an upper limit point and has to be selected carefully in order to obtain signal from the particle or cell (Nieuwenhuis et al. 2004; Gawad et al. 2004). In order words, the high frequency requires more consideration of the electrode design and signal processing. The capacitive measurement technique measures the AC capacitance instead of DC resistance when a particle passes the sensing electrodes. Thus, the capacitive measurement is particularly useful in the case of low electrical conductance liquids because it is very difficult to detect the resistance change resulted from the passage of a particle in an insulating solution. Other measurement techniques include inductive measurements (Du et al. 2010), metal-oxide-semiconductor field-effect transistor (MOSFET) which detects the particles by monitoring the MOSFET drain current modulation (Sridhar et al. 2008), radio frequency reflectometer, and capacitance measurements (Murali et al. 2008).

The objective of this paper is to develop a MEMS Coulter counter that can detect and monitor dynamic cell impedance changes and cellular volumetric changes as function of time and at various temperatures in response to mixing isolated cell populations with different extracellular media by using a sequence of ten electrode pairs. The cellular volumetric changes can be used to accurately determine cell-membrane permeability characteristics that can be used to significantly improve the efficacy of cryopreservation procedures and enhance the cell survival rates. We report the detection of yeast cells, red blood cells and microbeads with diameters between 7–20 μm using series of vertical electrodes and through impedance measurement. We also report cell mixing efficiency using a passive mixer, and focusing of cells using dielectrophoresis and hydrodynamic focusing.

2 Coulter design and modeling

The MEMS Coulter counter consists of three regions fluidic microchannels with passive mixing of the reagents with a

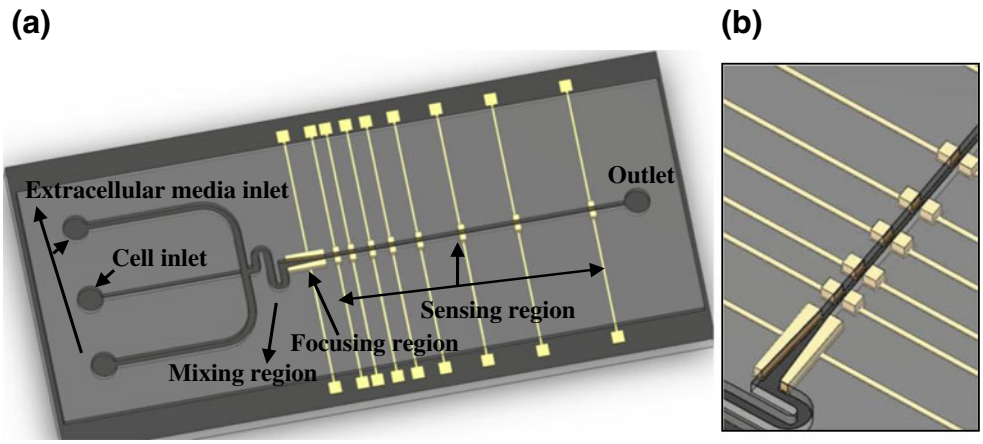

Fig. 1 (**a**) Schematics of the MEMS Coulter counter. The SU-8 channel and gold electroplated electrodes have thicknesses of 28 μm, and 25 μm, respectively. The mixing, focusing and measuring channels have width and length of 100 μm, 100 μm, 25 μm, and 0.3 mm, 0.8 mm, and 20 mm. respectively. The device top cover was not shown in the drawing, (**b**) A magnified view of the focusing and detection electrodes, and the Coulter channel

length of 0.4 mm; negative dielectrophoretic focusing of the cells using ramp down vertical electrode with a length of 0.9 mm; and an electrical impedance based sensing mechanism using a series of vertical electrode pairs with a total length of 20 mm (See Fig. 1). The cells are introduced via a single centered inlet while the extracellular media are introduced via two outer inlets into a T-shaped channel. The solution subsequently entered into a short serpentine shaped channel that mixes them further using chaotic advection and diffusion (Jiang et al. 2004). The intersection of the three channels along with the serpentine shape channel forms the mixing region. The mixing region is connected to the focusing region which consists of ramp down electrode pair that generates a non-uniform AC electric field and hence uses negative dielectrophoretic (DEP) forces in order to focus the cell into the center of the microchannel (low electric field) and directs them toward the Coulter counter microchannel (detection zone). This focusing region is then connected to the measuring region, and on to the outlet. The goal is to study how cell properties change as a function of time after they are exposed to a different extracellular media. This is accomplished by placing 10 electrode pairs along the Coulter channel such that each electrode pair records the impedance of cell at the time it passes through it. Thus, the impedance changes can be tracked as a function of time across the channel. It is important to note that the gradient of the fluidic medium in the mixing region will not impose any measurable bias on the downstream impedance measurements because the medium will mix completely and become homogeneous by the time it reaches the measuring region. Polydimethylsiloxane (PDMS) is chosen as a cover for the channel, due to its advantages such as flexibility, ease of fabrication, and transparency.

2.1 Design of mixing region

The MEMS Coulter counter is designed to monitor the cellular volumetric change after mixing the cell with different extracellular media within 0.3 s from the start of mixing and up to several seconds 5–10 s (Milgram and Solomon 1977; Papanek 1978). The volumetric changes of cells are due to the net movements of water between the cells and surrounding interstitial fluids, which are determined by the osmolalities of these two compartments (Macknight and Leaf 1977). If the osmolality of the interstitial fluid increases, water must leave the cells and, hence, cell volume decreases. *Vice versa*, fluid must enter the cells and the cell volume increases as osmolality decreases. Therefore, the cells should be mixed very well with specific extracellular media before their impedance are measured. The mixing region of the Coulter counter is designed with a passive mixer which allows chaotic mixing of different extracellular media and cells in a T-shaped channel and serpentine-shaped channel to achieve excellent fluid mixing efficiency. The passive mixer has two extracellular media channels with a width (150 μm) two times larger than the cell suspension flow channel (70 μm), and a vertical direction to the cell suspension flow channel in order to significantly improve the mixing efficiency. The serpentine shape mixer with a width of 100 μm is selected because it is relatively easy and simple to implement. The mixing capability of the Coulter counter was simulated using COMSOL finite

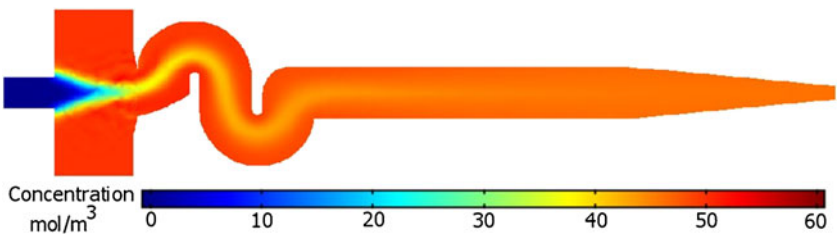

Fig. 2 Simulation of mixing two dyes with different colors in the Coulter counter channel

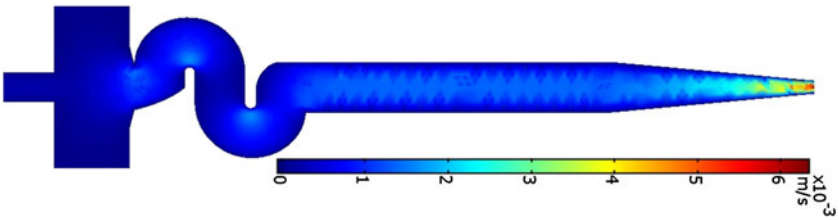

Fig. 3 3-D simulation of fluids velocity in the micromixer

element tool under steady-state condition. The fluid flow was assumed to be laminar and incompressible, and the boundary is non-slip. A concentration of 50 mol/m^3 was set to the two outer inlets (red in color) while the center inlet (blue in color) was set to 0. The isotropic diffusion coefficient of substance in the water was set to $1\times e^{-10}$ m^2/s. A fixed pressure of 6 Pa was applied to the two inlets in order to achieve similar flow rate of 0.5 μl/min. The quality of mixing was evaluated by observing color intensity variation as they were flowing through the mixer and just before they enter to the Coulter channel (See Fig. 2). The uniform orange color at right side of the focusing channel is an excellent indication of a complete mixing. The mixing efficiency is an important factor that determines the sensitivity of the system and can be determined experimentally by analyzing captured optical images after mixing using image processing. The fluid velocity in the center of the channel was varied between 2.5 mm/s and 6 mm/s which correspond to a mixing time of 0.3 s (See Fig. 3).

2.2 Design of cell focusing region

The cell focusing region consists of a vertical ramp down electrode pair with a ramp down channel that employs negative DEP and hydrodynamic focusing to focus the cells into the center of the microchannel in line in order to prevent clogging the Coulter channel. The vertical ramp down electrode pair is simulated using COMSOL as shown in Fig. 4.

The results show that the electric field intensity is decreasing towards the center of the channel. Thus, the cell can be directed and focused into the center of the microchannel. The arrows point in the direction of the gradient of the electric field, corresponding to the direction of DEP force. Sizes of the arrows are proportional to the intensity of the electric field gradient which is a factor of the DEP force (Fig. 4(a)). A three-dimensional view of trace of the particle‘s movements with one starting from the bottom left corner of the inlet and the other starting from the bottom right corner of the inlet (Fig. 4(b)). The virtual particle mass is 1.44×10^{-12} kg which is the approximate mass of a sphere with diameter 10 μm was put in the model with an initial velocity of 2 m/s in axial direction. The dielectric constant and conductivity of the particle were set to 2.5 and 10^{16} S/m. The dielectric constant and conductivity of the medium were set to 80 and 0, respectively, which are the same as the water. Both of them left the outlet close to the central point. Obviously, the DEP forces changed the direction and velocity of the particle directing it to the center of the microchannel.

2.3 Design of detection zone

The detection zone consists of series of 10 gold electroplated vertical electrode pairs. The use of vertical electrode design will generate a uniform E-field over the entire height of the microchannel along the direction perpendicular to the

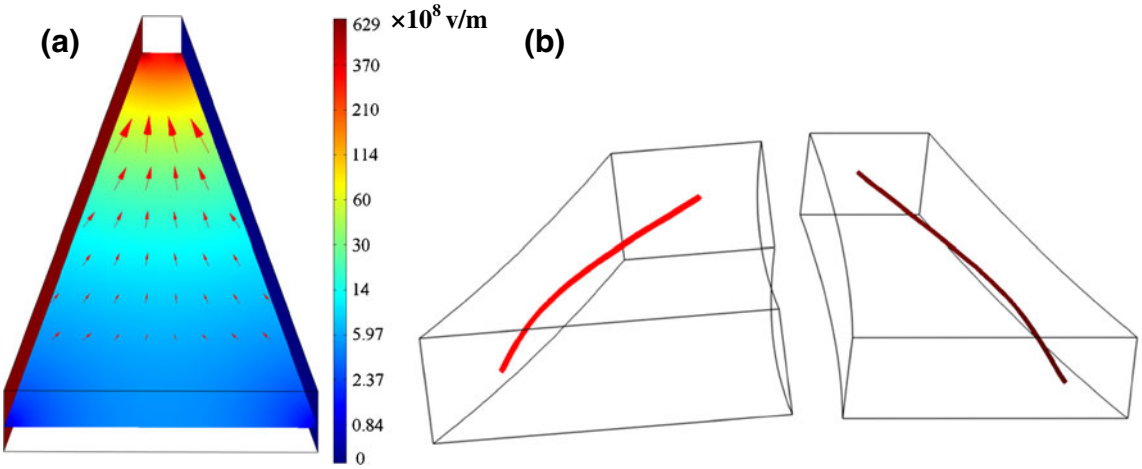

Fig. 4 (**a**) Simulation of electric field and its gradient distribution in ramped-shape DEP electrodes, (**b**) Two particle movement traces under influence of DEP forces. Left: from top left of entrance; Right: from bottom right of entrance

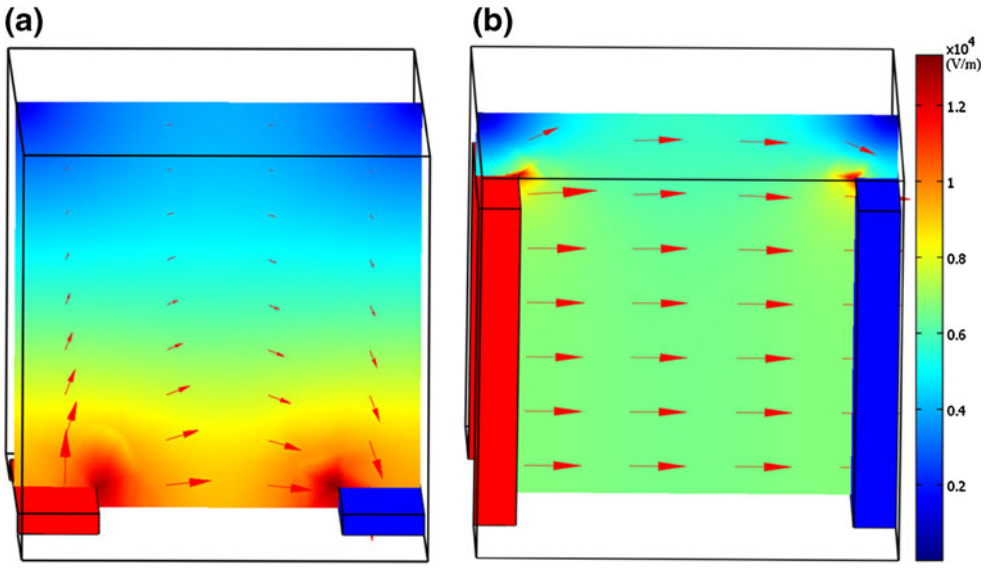

Fig. 5 Comparision of electric field simulation generated by (**a**) thin film electrodes and (**b**) vertical electrodes. The arrows point towards the direction of the electric field and their size along with the colors are proportional to the intensity of the electric field

channel, as illustrated with a uniform color and same size arrows in Fig. 5. Thus, this will increase the measurement sensitivity. The distribution of electrodes along the channel was designed such that measurements are made more frequently at the beginning, during the most transient phase of cell volume change. Impedance of cells was monitored along the whole channel as cells pass through. Traditionally, the MEMS based Coulter counter employed thin films of electrodes patterned underneath and across the microchannel (Fig. 5(a)). This configuration generates non-uniform electric-field along its vertical direction (Chang et al. 2007; Chen and Wang 2008), and is highest at the electrode surfaces and diminish away from them which will reduce the detection sensitivity considerably (Fig. 5(b)). Thus, those devices generate signal variations if identical particles pass at different heights over the electrodes.

3 Device fabrication

The device was fabricated on top of a glass substrate using a series of surface micromachining, photolithography, SU-8 photoresist and PDMS processes in the following sequence (See Fig. 6). 1) The glass slides were cut into an appropriate size to fit one device. They were then cleaned using a piranha solution which consists 3:1 ratio of sulfuric acid and hydrogen peroxide (H_2SO_4: H_2O_2) for 3 min in order to remove the organic contamination, then washed

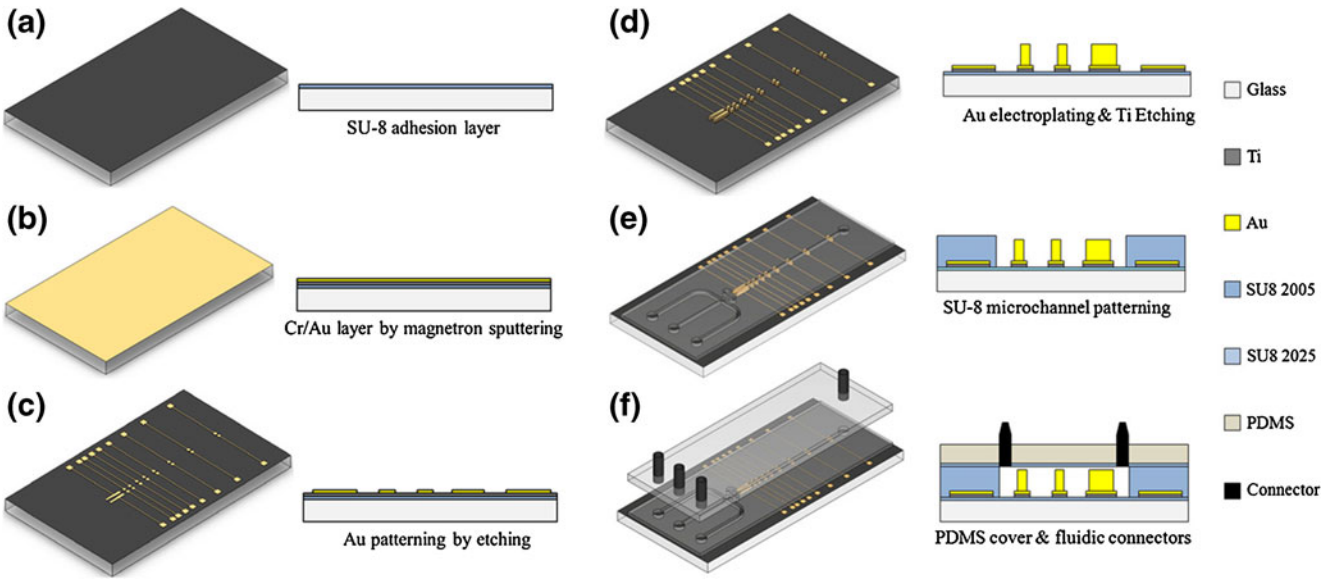

Fig. 6 Side view of the Coulter counter fabrication process flow

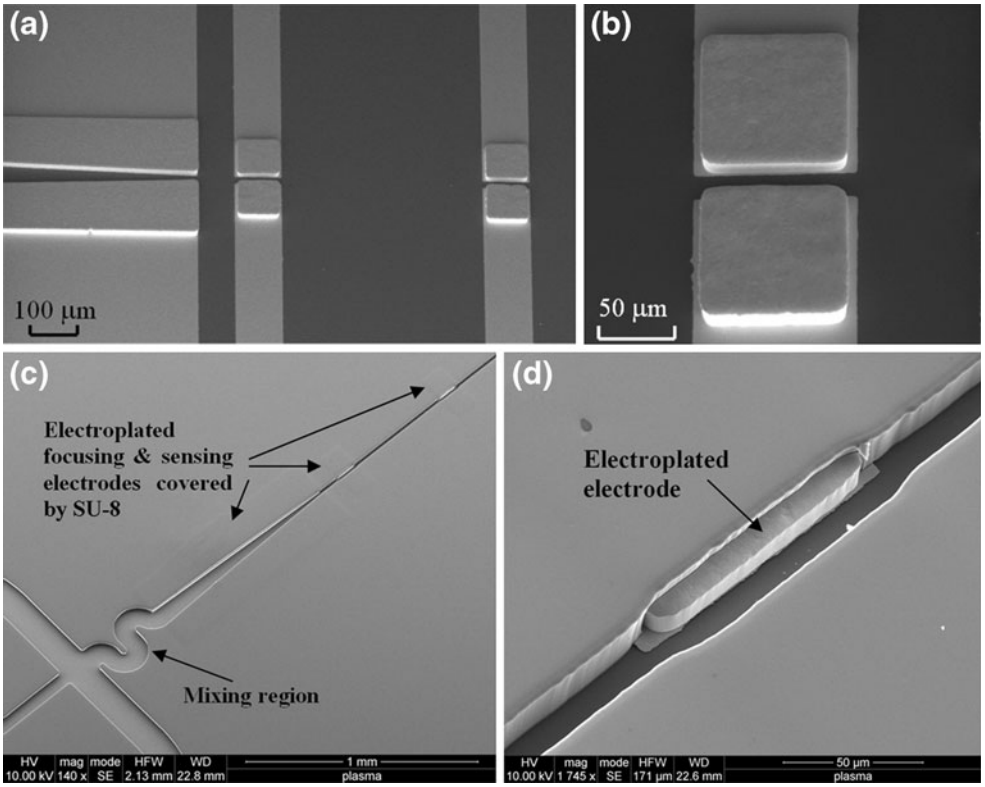

Fig. 7 SEM images of (**a**) gold electroplated focusing and detection electrodes, (**b**) magnified view of the one detection electrode pair, (**c**) the Coulter counter without top cover. The micrograph shows the SU-8 microchannels, mixing region, focusing electrodes and couple of sensing electrodes, (**b**) magnified view of one sensing electrode and the Coulter Channel

thoroughly with DI water and dried with a nitrogen blower. 2) Immediately after the cleaning, a layer of SU-8 photoresist (Microchem 2005) with a thickness of 4 μm was spin coated onto the glass slides followed by a UV flood exposure without masking. The substrate was then hard baked at 150°C for 30 min to completely cure SU-8 layer (Fig. 6 (a)). This additional layer of SU-8 improved the adhesion between the following SU-8 (Microchem 2005) channel and glass substrate and thus preventing it from peeling off from the substrate. 3) Two layers of titanium (Ti) and gold (Au) were deposited with a thickness of 40 nm and 140 nm, respectively, using magnetron RF sputtering at 4 mTorr. These layers served as the seed layer for electroplating. Gold layer was patterned using wet etching in potassium iodide (KI) and iodine (I_2) mixture in order to create the electrode traces, bonding pads and seed layer for electroplating the focusing and sensing electrodes (Fig. 6(b)). 4) A photoresist mold (AZ 4620) with a thickness of 25 μm was formed by double spin coating for electroplating the vertical electrodes. The electrodes were created by electroplating gold inside the mold with a thickness of 25 μm (Fig. 6(c)). 5) The photoresist was washed away and the Ti layer was wet etched using buffered hydrofluoric acid (Fig. 6(d)). 6) The microchannel was defined using SU-8 (Microchem 2025) with a thickness of 28 μm (Fig. 6(e)). The SU-8 microchannel was then treated to improve its biocompatibility. It was first exposed to 450 mJ/cm^2 UV flood for 1 h followed by 150°C oven baking for 24 h. It was finally exposed to oxygen plasma for 20 s and isopropanol (IPA) wash for 1 min. 7) The PDMS slabs were made and cured to serve

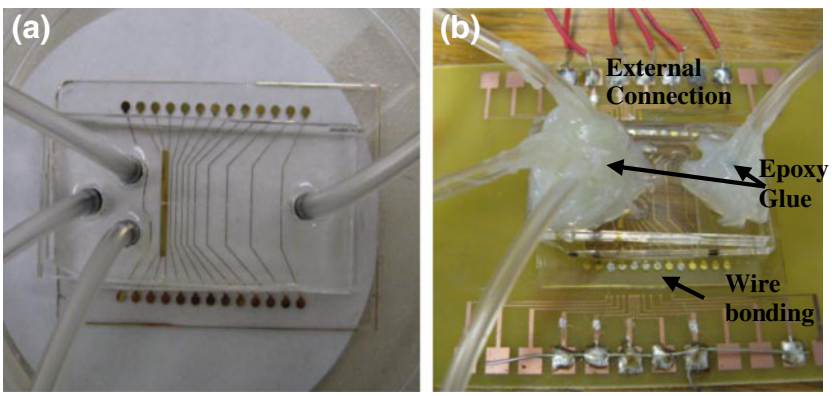

Fig. 8 The optical images show (**a**) a complete fabricated and packaged Coulter counter device with PDMS Cover, and fluidic connectors, (**b**) the same device but sealed with epoxy glue

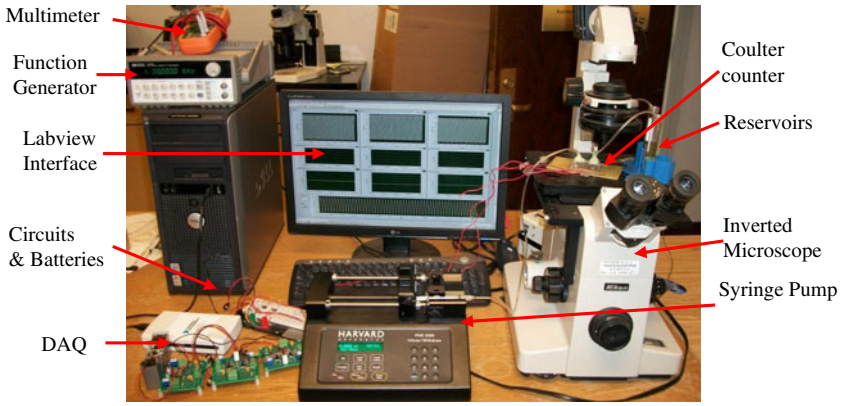

Fig. 9 An optical photo of the experimental setup is shown. The device was placed on an inverted microscope and its inlets and outlet were connected to a syringe pump and reservoirs. The electrodes were connected to printed circuit board and computer via Labview data acquisition board. The function generator was used for excitation and measurements from the focusing electrodes

as top cover along with fluidic connectors (fluidic inlets and outlets). 8) An oxygen plasma treatment was applied on the PDMS cover in order to change its surface to hydrophilic and then SU-8 was spin coated onto it and oven baked at 95° C for 10 min to serve as glue. The oxygen plasma step was used to improve the adhesion of SU-8 to PDMS. 9) The microchannel was then aligned and bonded to the PDMS/SU-8 cover manually and baked on a hotplate at 48 ◦C for 1 h while a pressure is applied to secure the bonding. The PDMS/SU-8 cover and SU-8 microchannel were cross-linked and formed a strong bond (Fig. 6(f)). During the bonding process, it was found that lower bonding temperature would cause weak bonding and air bubbles were trapped in the interface, and the higher bonding temperature would cause SU-8 to flow into the microchannel and block it. The optimized bonding temperature was between 45–50°C.

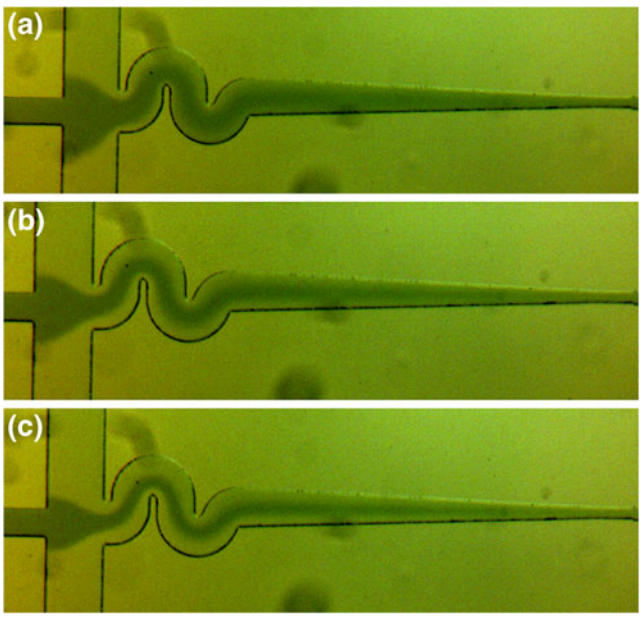

Fig. 10 Bottom views of the mixing efficiency testing at three different flow rates of (**a**) 0.1 μl/min, (**b**) 0.4 μl/min, **c**) 0.8 μl/min. The quality of mixing was evaluated optically by observing color intensity variation of the two colorful fluids as they are flowing through the mixer and just before focusing region

This is followed by UV flood exposure (450 mJ/cm^2) and hard baking at 120°C for 20 min in order to fully cure the SU-8 layer. 10) The fluidic connectors are further sealed by epoxy glue in order to improve the device reliability and eliminate any possible fluid leakage. 11) In the last step, the device was fixed and wire bonded to PCB for external electrical connections. Optical images and magnified view of the fabricated device along with a complete device with wire bonding, packaging and soldering for external connections are shown in Figs. 7 and 8.

4 Testing and results

4.1 Experimental set up

The experimental setup for characterizing the fabricated coulter counter is shown in Fig. 9. A syringe pump (a Harvard Apparatus PHD 2000) was used to inject fluid at different volumetric flow rates. A CCD camera installed on an inverted microscope was used to capture optical images of the device during experiment. An electrical circuit is designed and built in order to measure the impedance

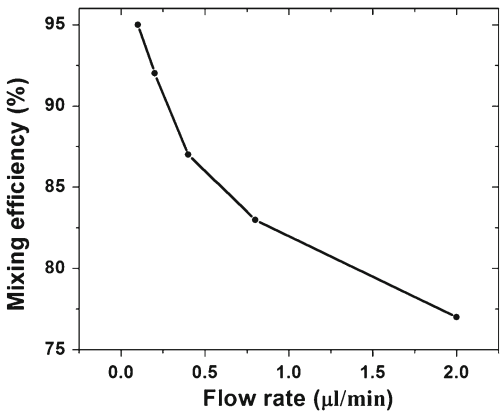

Fig. 11 The mixing efficiency of passive micromixer is plotted as a function of flow rate. In actual cell study experiment, a flow rate of 0.5 μl/min was chosen to reach desired fluids velocity which corresponds to a mixing efficiency of 85 %

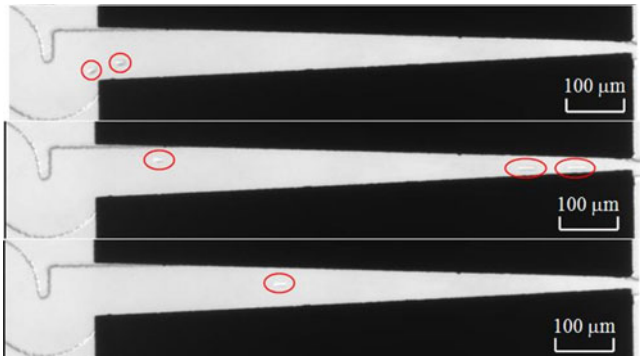

Fig. 12 Three sequential images (bottom view) captured by a CCD camera to demonstrate focusing capability of the device

changes of microbeads and cells in the measuring region. Labview system and data acquisition board (DAQ) USB-6216 (National Instrument, Austin, TX) were employed in order to record large volume of data from 10 channel and thus, enable tracking the impedance of same Yeast and red blood cells by 10 pairs of electrodes as they flow through the detection microchannel.

4.2 Mixing of fluids in the channel

The mixing efficiency of the Coulter counter was determined by flowing two fluids with different colors into the device. Black dyed water was introduced via a single centered inlet while deionized water was introduced via two outer inlets into a T-shaped channel. As soon as the two fluids reached the T-intersection, they start to mix. The two fluids subsequently entered into a short serpentine shaped channel that mixed them further using chaotic advection and diffusion. The mixing continued in the focusing region until it was complete just before the first detection electrode. The quality of mixing was evaluated optically by observing color intensity variation of the two colorful fluids as they are flowing through the mixer and just before focusing region. Optical images of mixing of the two colorful fluids at different flow rates are shown in Fig. 10. These optical images were converted to grayscale images and were used to extract the mixing efficiency. To quantitatively evaluate the mixing efficiency, we first calculated the standard deviation (σ) of a narrow strip across the entrance of the Coulter channel (before the first impedance measurement) using Matlab and is given by:

$$\sigma = \sqrt{\frac{1}{N}\sum_{i=1}^{N}(I_i - I_{mean})^2}$$

where I_i and I_{mean} are intensity the i^{th} pixel and average intensity of the whole narrow strip across the channel, respectively, and N is the total number of pixels within the narrow strip area. The mixing efficiency (C_{mix}) is calculated by normalizing the standard deviation (σ) with respect to the standard deviation at the junction of the three inlets (σ_{inlet}) where no mixing took place (Nguyen et al. 2008).

$$\mathrm{C_{mix}} = \frac{\sigma_{inlet} - \sigma}{\sigma_{inlet}} \times 100\%$$

The calculated mixing efficiency at various flow rates are shown on Fig. 11. It was varied from 77 %–95 % by varying the fluidic flow rate from 4–0.1 μl/min, respectively. For example, a mixing efficiency of 87 % was achieved with a flow rate of 0.4 μl/min. We have selected a 0.5 μl/min which corresponds to a mixing efficiency of 85 %.

This value was selected in cell study measurements as a trade-off between mixing time and mixing efficiency. With this flow rate, we achieved sufficient mixing and a velocity of 3.4 m/s which correspond to a time span between the start of mixing and the first impedance measurement of 0.3 s. It is important to note that the use of T-shaped channel with narrower cell center channel have improved our mixing efficiency without compromising the mixing time. In future experiment, the outer channel will be made four times wider than the center channel, and the focusing region channel width will be reduced by 20 % to 80 μm. These modifications will increase the mixing efficiency to 100 % and decrease the mixing time to 0.2 s.

4.3 Focusing electrode testing

The quality of focusing microbeads to the center of the microchannel was tested by applying AC electric field across DEP electrodes. Latex microbeads with nominal diameter of 10 μm placed inside DI water container and were flown into the device. A sinusoidal voltage with amplitude of 6 V (peak-to-peak) at 10 MHz frequency was

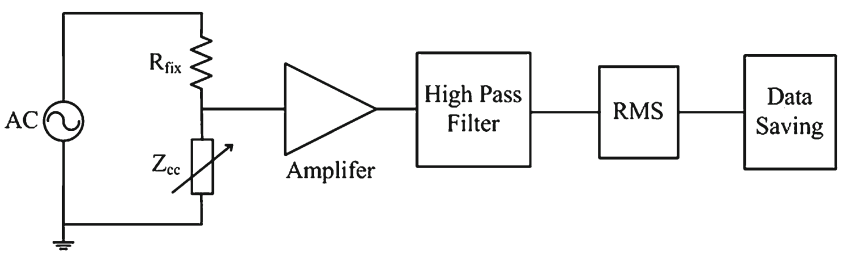

Fig. 13 Electrical testing circuit for measuring signal from one channel

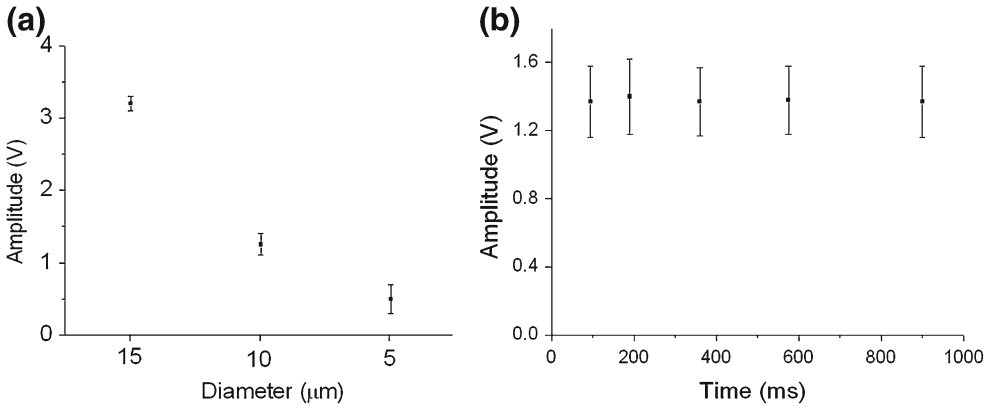

Fig. 14 The figures show (**a**) voltage pulses with different amplitude which corresponds to microbeads with diameters of 5 μm, 10 μm & 15 μm, (**b**) the impedances of a single microbeads with a diameter of 15 μm that were recorded using 6 electrode pairs. Standard deviation is shown by error bar

applied to the focusing electrodes. Figure 12 shows sequential images that demonstrate the movements and focusing of three latex microbeads. The black areas in the image are bottom views of the DEP electrodes. The microbeads are flowing from the mixing region (left) to the focusing region, and exited to the impedance measuring region (right). It is important to note that it is not clear from this experiment whether the microbeads were focused by DEP forces or by hydrodynamic forces or by both forces combined. The short length of the focusing channel (0.8 mm) which corresponds to a focusing time of 0.235 s is too small to enable the observation of microbead movements under the microscope. Thus, a high speed camera might be needed for future testing to capture fast moving microbeads or cells.

4.4 Electrical testing

Prior to assessing the fabricated and packaged Coulter counter devices, an electrical circuit was designed and built in order to measure the impedance changes of cells and microbeads in the measuring region as shown in Fig. 13. The circuit consists of a voltage divider, an amplifier, high pass filter and Labview interface for data acquisition. An AC signal source was used and root mean square (RMS) value was taken as the signal amplitude. The signals were measured as voltages and then were converted back to impedances using electrical circuits which include voltage dividers, band pass filter, instrumentation amplifiers, and second order Butterworth high pass filters in Labview:

$$\frac{\Delta Z}{Z_{ch}} = \frac{\frac{\Delta V}{G_{amp}}}{V_{ch}}$$

where V_{ch} is the baseline voltage of the channel signal, ΔV is the voltage change caused by a cell or particle in the channel, Z_{ch} is the base impedance without a cell or a particle in the channel, ΔZ is the impedance change caused by a cell or a particle in the channel and G_{amp} is the gain of the instrumentation amplifiers. The baseline voltage and base impedance of the channel can be measured and estimated at the voltage divider. The conversion is valid with the assumption that all filters and amplifiers have the ideal characteristics and frequency responses. Another assumption is made that the reactance of the channel impedance is negligible and ratio of ΔZ to Z_{ch} is very small.

The MEMS based Coulter counter performance was tested as a function of time using an AC voltage source. In the first experiment, latex microbeads with diameters of 5 μm, 10 μm and 15 μm, and saturated with saline water were injected into the microchannel via the three inlets and measured using a series of 6 electrode pairs. The measured impedances of the three microbeads sizes, using the same

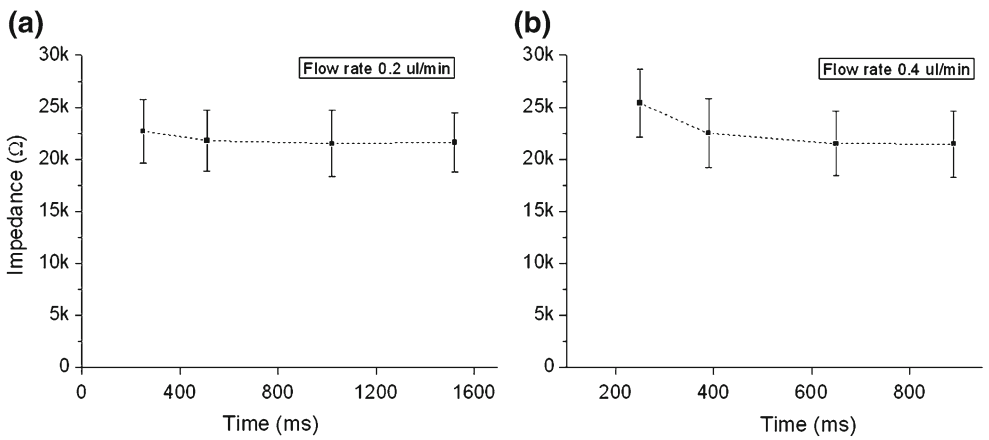

Fig. 15 Impedances changes of yeast cells after mixing with DMSO at flow rates of (**a**) 0.2 μl/min, (**b**) 0.2 μl/min

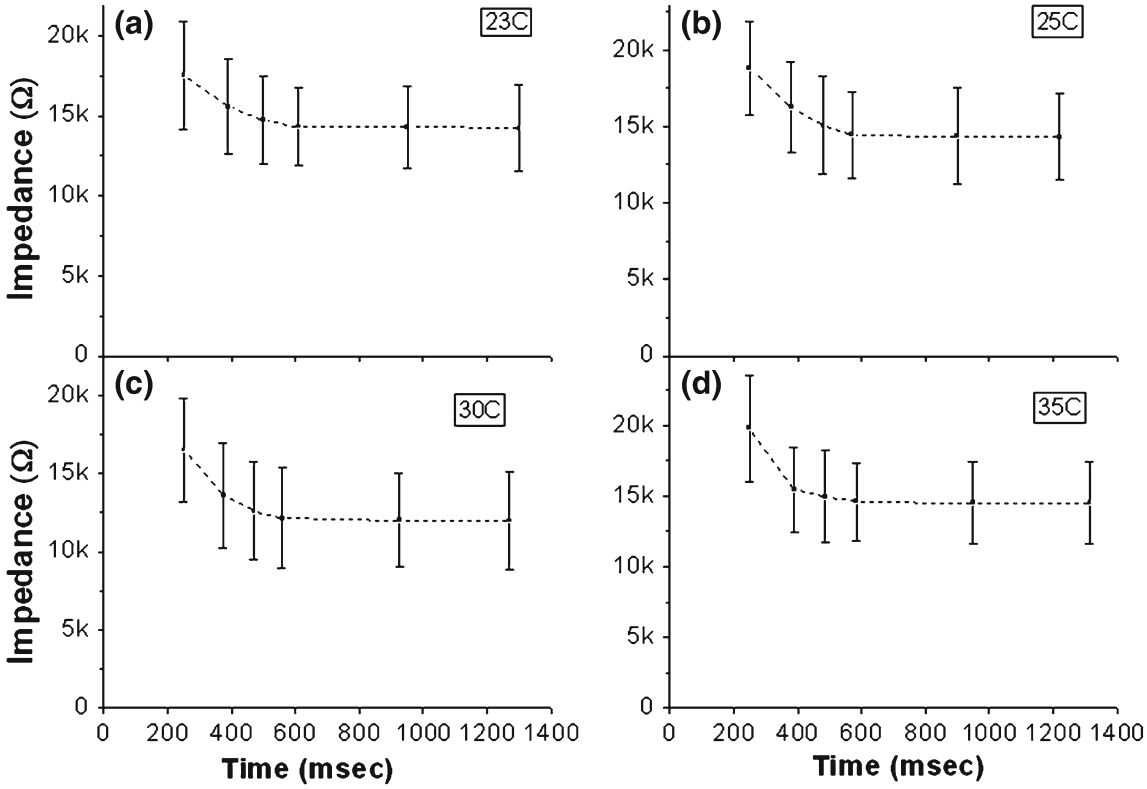

Fig. 16 Impedances changes of yeast cells after mixing with DMSO measured at different temperatures (**a**) 23°C, (**b**) 25°C, (**c**) 30°C, (**d**) 35°C

electrode pair, have three different amplitudes as shown in Fig. 14(a). This demonstrates the device ability to differentiate between cells and beads based on their size and also count them. The measurement results also demonstrate that the impedances of a single microbead that were recorded using 6 electrode pairs have same impedance value. This is expected since the cell volume would not change (See Fig. 14(b)). The error bar on the figure demonstrates a very small standard deviation of the signals measured by each electrode pair.

In the second experiment, yeast cells were injected into center channel while the cryoprotective agent dimethyl sulfoxide $(CH_3)_2SO$ (DMSO) which was diluted to 4 % with DI water to achieve an osmolality of 600 mmol/kg solution, was injected into the outer two channels. The device was tested at several flow rates at room temperature in order to determine the most appropriate flow rate that can achieve an excellent mixing within 0.3 s from the start of mixing. The measured impedances of yeast cells at 0.2 μl/min and 0.4 μl/min flow rate were shown in Fig. 15. The results demonstrate that a flow rate of 0.4 μl/min achieve excellent mixing efficiency within 0.3 s. Thus, the most transient phase of cell volume changes was observed within 0.6 s from the start of mixing. In addition, this experiment confirms that mixing efficiency determined by modeling is accurate and satisfactory. Therefore, we have chosen a flow rate of 0.4 μl/min in the following experiments.

The impedances of yeast cells were measured again at 23°C, 25°C, 30°C and 35°C using flow rate of 0.4 μl/min (See Fig. 16). The results show the impedance of yeast cells decreases for the first 4 electrodes and then start to stabilize, which indicates that the cells are saturated. The total time that it took cells to stabilize after mixing is 0.6 s. The results also indicate that at elevated temperature yeast cells shrink a little bit more and faster than at lower temperature. The error bars on the figure show small fluctuation in impedance.

In the third experiment, Red blood cells in PBS 1x was injected into the center inlet while DI water was flown into outside 2 inlets with a flow rate. The impedances of RBCs were measured using 5 electrode pairs at 0.4 μl/min flow rate and are shown in Fig. 17. The impedance of cells starts to increase at the first 3 electrodes and then starts to level

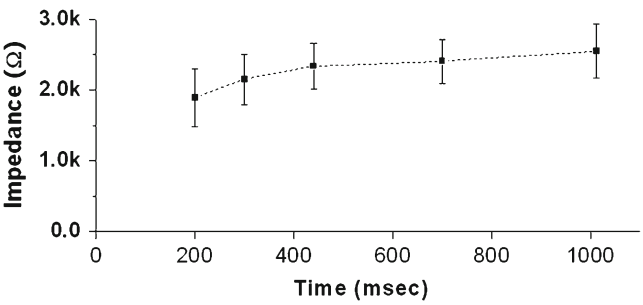

Fig. 17 Red blood cells in phosphate buffer solution 1x were mixed with DI water. Standard deviations are shown by error bars

off. The increase in impedance is due to the increase in cell volume and the leveling off is indicates the cell volume is saturated. It is important to note that the low value of RBC impedance due to the small size cells in comparison with the Coulter channel dimension. Thus, in order to obtain a higher resolution signal, the Coulter channel dimension should be reduced to a size close to the cell diameter.

Each sampling point of those set of experiments was consisted of 25 samples of microbeads or cells. After each experiment, *T*-test was conducted to assess whether the mean of two consecutive sampling points were statistically different from each other. All the calculated T-tests p-values were smaller than 0.05 which indicates their means were statistically different from each other.

5 Conclusions

A novel MEMS Coulter counter has been designed for measuring the dynamics of single cell volume in response to mixing with various agents. The device uses passive mixing, the phenomenon of dielectrophoresis to focus the cells to the center of the channel, and Coulter principle to detect cells based on the change in impedance when they pass through the sensing zone. The fluidic testing which include mixing and focusing demonstrate sufficient mixing and satisfactory focusing. The electrical testing were performed using latex microbeads with diameters of 5 μm, 10 μm and 15 μm, yeast cells and red blood cells with dynamic volumes changes, validate the performance of the device. The device has the potential to provide data enabling the development of a mathematical model to describe the reaction of CPA and cells in cryopreservation.

References

D.A. Ateya, J.S. Erickson, P.B. Howell Jr., L.R. Hilliard, J.P. Golden, F.S. Ligler, The good, the bad, and the tiny: a review of micro flow cytometry. Anal. Bioanal. Chem. **391**, 1485–1498 (2008)

R. Bernini, E.D. Nuccio, F. Brescia, A. Minardo, L. Zeni, P.M. Sarro, R. Palumbo, M.R. Scarfi, Development and characterization of integrated silicon micro flow cytometer. Anal. Bioanal. Chem. **386**, 1267–1272 (2006)

C.C. Chang, Z.X. Huang, R.J. Yang, Three-dimensional hydrodynamic focusing in two-layer polydimethylsiloxane (PDMS) microchannels. J. Micromech. Microeng. **17**, 1479–1486 (2007)

H.T. Chen, Y.N. Wang, Fluorescence detection in a micro flow cytometer without on-chip fibers. Microfluid Nanofluid **4**, 689–694 (2008)

H.T. Chen, Y.N. Wang, Optical microflow cytometer for particle counting, sizing and fluorescence detection. Microfluid Nanofluid **6**, 529–537 (2009)

W.H. Coulter, US Patent 2,656,508 (1953)

L. Du, J. Zhe, J.E. Carletta, R.J. Veillette, Inductive Coulter counting: detection and differentiation of metal wear particles in lubricant. Smart Mater. Struct. **19**, 057001 (2010)

J.M. England, M.C. Down, Measurement of the mean cell volume using electronic particle counters. Br. J. Haematol. **32**, 403–410 (1975)

F.U. Gast, P.S. Dittrich, P. Schwille, M. Weigel, M. Mertig, J. Opitz, U. Queitsch, S. Diez, B. Lincoln, F. Wottawah, S. Schinkinger, J. Guck, J. Kas, J. Smolinski, K. Salchert, C. Werner, C. Duschl, M.S. Jager, K. Uhlig, P. Geggier, S. Howitz, The microscopy cell (MicCell), a versatile modular flow through system for cell biology, biomaterial research, and nanotechnology. Microfluid Nanofluid **2**, 21–36 (2006)

S. Gawad, L. Schild, P. Renaud, Micromachined impedance spectroscopy flow cytometer for cell analysis and particle sizing. Lab-on-a-Chip **1**, 76–82 (2001)

S. Gawad, K. Cheung, U. Seger, A. Bertsch, P. Renaud, Lab Chip **4**, 241–251 (2004)

D. Holmes, H. Morgan, N.G. Green, High throughput particle analysis: combining dielectrophoretic particle focusing with confocal optical detection. Biosens. Bioelectron. **21**, 1621–1630 (2006)

F. Jiang, K.S. Drese, S. Hardt, M. Kupper, F. Schonfeld, Helical flows and chaotic mixing in curved micro channels. A.I.Ch.E. J **50**, 2297 (2004)

M. Koch, A.G.R. Evans, A. Brunnschweiler, Design and fabrication of a micromachined Coulter counter. J. Micromech. Microeng. **9**, 159–161 (1999)

D. Larsen, G.B. Lankenstein, J. Branebjerg, Microchip coulter particle counter. Transducers'97, 1319–1322 (1997)

S.W. Levin, R.L. Levin, A.K. Solomon, A. Pandiscio, D.H. Kirkwood, Improved stop-flow apparatus to measure permeability of human red cells and ghosts. J. Biochem. Biophys. Meth. **3**, 255–272 (1980)

C. Lin, G. Lee, L. Fu, B. Hwey, Vertical focusing device utilizing dielectrophoretic force and its application on microflow cytometer. IEEE Trans. J. MEMS **13**, 923–932 (2004)

A.D.C. Macknight, A. Leaf, Regulation of cellular volume. J. Physiology **57**, 510–73 (1977)

X. Mao, J.R. Waldeisena, T.J. Huang, Microfluidic drifting implementing three-dimensional hydrodynamic focusing with a single-layer planar microfluidic device. Lab-on-a-Chip **7**, 1260–1262 (2007)

J.H. Milgram, A.K. Solomon, Membrane-permeability equations and their solutions for red-cells. J. Membr. Biol. **34**, 103–144 (1977)

S. Murali, X. Xia, A.V. Jagtiani, J. Carletta, J. Zhe, Capacitive Coulter counting: detection of metal wear particles in lubricant using a microfluidic device. Smart Mater. Struct. **18**, 037001 (2008)

T.N.T. Nguyen, M.C. Kimb, J.S. Park, N.E. Lee, An effective passive microfluidic mixer utilizing chaotic advection. Sensor Actuator B Chem. **132**, 172–181 (2008)

J.H. Nieuwenhuis, F. Kohl, J. Bastemeijer, P.M. Sarro, M.J. Vellekoop, Integrated Coulter counter based on 2-dimensional liquid aperture control. Sensor Actuator B Chem. **102**, 44–50 (2004)

T. Papanek, The water permeability of the human erythrocyte in the temperature range +25 C to −10 C, PhD thesis, Massachusetts Institute of Technology (1978)

O.A. Saleh, L.L. Sohn, An artificial nanopore for molecular sensing. Nano Lett. **3**, 37–38 (2003)

R. Scott, P. Sethu, C.K. Harnett, Three-dimensional hydrodynamic focusing in a microfluidic Coulter counter. Rev. Sci. Instrum. **79**, 046104 (2008)

M. Sridhar, D. Xu, Y. Kang, A.B. Hmelo, L.C. Feldman, D. Li, D. Li, Experimental characterization of a metal-oxide-semiconductor field-effect transistor-based Coulter counter. J. Appl. Phys. **103**, 104701 (2008)

N. Sundararajan, M.S. Pio, L.P. Lee, A. Berlin, Three-dimensional hydrodynamic focusing in Polydimethylsiloxane (PDMS) microchannels. IEEE Trans. J. MEMS. **13**, 559–567 (2004)

C. Tsai, H. Hou, L. Fu, An optimal three-dimensional focusing technique for micro-flow cytometers. Microfluid Nanofluid **5**, 827–836 (2008)

Z. Wang, O. Hansen, P.K. Petersen, A. Rogeberg, J.P. Kutter, D.D. Bang, A. Wolff, Dielectrophoresis microsystem with integrated flow cytometers for on-line monitoring of sorting efficiency. Electrophoresis **27**, 5081–5092 (2006)

J. Zhe, A. Jagtiani, P. Dutta, H. Jun, J. Carletta, A micromachined high throughput Coulter counter for bioparticle detection and counting. J. Micromech. Microeng. **17**, 304 (2007)

S. Zheng, Y.C. Tai, Design and fabrication of a micro coulter counter with thin film electrodes. Proceedings of 2006 International Conference on Microtechnologies in Medicine and Biology. 16–19 (2006)

S. Zheng, M. Liu, Y.C. Tai, Micro coulter counters with platinum black electroplated electrodes for human blood cell sensing. Biomed. Microdev. **10**, 221–231 (2008a)

S. Zheng, M.S. Nandra, C.Y. Shih, W. Li, Y.C. Tai, Resonance impedance sensing of human blood cells. Sensor Actuator Phys. **145**, 29–36 (2008b)

S. Zheng, Y.C. Tai, Design and fabrication of amicro coulter counter with thin film electrodes. Proceedings of 2006 International Conference on Microtechnologies in Medicine and Biology. 16–19 (2006c)